Polymer Bulletin 41, 341–348 (1998)

Polymer Bulletin

AFM study of lamellar thickness distributions in high temperature melt-crystallization of ß-polypropylene

D. Trifonova [1], J. Varga [2], G. J. Vancso [1,*]

[1] Faculty of Chemical Technology, University of Twente, P.O.Box, 7500 AE Enschede, The Netherlands
[2] Friedrich-Alexander Universität, Erlangen-Nürnberg, Lehrstuhl für Kunststofftechnik, D-91058 Erlangen, Germany

Received: 2 February 1998/Revised version: 10 July 1998/Accepted: 11 July 1998

Summary
Atomic force microscopy (AFM) was used to study the lamellar thickness and its distribution in the ß modification of isotactic polypropylene-(ß-iPP) crystallized from the melt at high temperatures. Measurements were performed on lamellae oriented both flat-on and edge-on with respect to the examined surface. Average lamellar thickness was found to be dependent not only on the crystallization temperature, but also on factors such as nucleation density and isothermal lamellar thickening. The limitations and advantages of the AFM technique for evaluation of lamellar thickness are discussed.

Introduction

The thickness of the lamellae in melt-crystallized polymers is a quantity which greatly influences their physical properties (1). This thickness depends on a variety of parameters and its value is often required in order to test crystallization theories (2). In the literature there have appeared a number of investigations in which different methods have been applied to determine the lamellar thickness and its distribution (3-19). The techniques which have been employed in these studies have included X-Ray scattering (3-8), Raman spectroscopy (9-12), and electron microscopy (13-16). Frequently, the results obtained by various techniques have differed, thus uncertainties remain surrounding the values of lamellar thickness for melt-crystallized polymers. The applicability of these methods, their limitations, and the interpretation of the results obtained have been discussed in detail by Dlugosz et al. (17) and Voigt-Martin and Mandelkern (18-19). It has been shown that the numerical estimation of the lamellar thickness and long spacing is a complex problem and depends on details such as crystal morphology and the nature of the thickness distribution (18-19).
AFM was established during the last ten years as a useful tool for the investigation of topology and physical characteristics of polymer surfaces (20). As in the case of electron microscopy, AFM has the advantage over averaging techniques such as X-Ray scattering and Raman spectroscopy of direct visual observation of the lamellar morphology. Furthermore it permits measurements of the lamellar thickness in real space. It has been shown that AFM can be used for measurements of the height of growth spiral terraces of polymer single crystals (21-23). This value cannot be determined by electron microscopy. Lamellar thickness distributions based on AFM measurements have also been reported (24-26). These measurements have been performed mainly on lamellae having their side surfaces exposed on the investigated surface (so-called “edge-on” view).

* Corresponding author

In the present study, AFM was applied to the estimation of the lamellar thickness and its distribution in ß-iPP crystallized from melt. The limitations and advantages of this technique for quantitative evaluation of lamellar thickness are discussed. The lamellar morphology and spherulitic structure of melt-crystallized i-PP have been extensively investigated by optical microscopy (27,28), transmission (29-34) and scanning (35,36) electron microscopy. The α (monoclinic) form has attracted the most attention, since when processed in laboratory or on an industrial scale iPP crystallizes predominantly in this form (37). The unique cross-hatched lamellar pattern, typical for monoclinic i-PP, has not been seen in any other polymer. The ß-iPP form has been observed in a much narrower temperature range and it cannot be produced in pure form without added nucleant (27,37). Elucidation of the structure of ß-iPP has been a considerable challenge. From its discovery it was clear that the structure had some kind of hexagonal symmetry. The model suggested in 1968 by Turner-Jones and Cobbold (38) of a hexagonal unit cell with parameters a = b = 19 Å, c = 6.5 Å was until recently widely accepted. This large cell included nine chains, and it was not clear how such a large number of chains can be arranged in a unit cell. In 1994 Meille *et al.* (39) and Lotz *et al.* (40) independently reached another structural solution for ß-iPP: a trigonal unit cell with parameters a = b = 11.01 Å, c = 6.5 Å, containing three isochiral helices. An essential characteristic of this structure is that it is frustrated (40). The "hexagonal" reciprocal lattice symmetry and the formation of quasi-hexagonal lamellae can be satisfactorily accounted for by this model.

In recent years there has been growing interest in the morphology of ß-iPP. Due to the identification of more efficient nucleating agents (41), it became possible to study in more detail the high-temperature crystallization of ß-iPP (36,42). Previously, the spherulitic crystallization of ß-iPP was restricted to high supercooling since its formation was detectable only under these conditions (36). In this report attention is focused on ß-iPP crystallized at temperature, near to the reported upper temperature limit of nucleation of this form (36,37).

Experimental

The i-PP homopolymer used in this study was Tipplen H523 (Tisza Chemical Works, TVK, Tiszaujvaros, Hungary), having M_w = 5.2 x 10^5 g/mol and M_n = 3.1 x 10^5 g/mol. Dehydrated calcium pimelate (41) (concentration between 0.01 to 0.5 percent by weight) was used to produce the ß modification of iPP. Samples, *ca.* 100 μm thick, were prepared between glass slide and cover slip. They were heated to 220°C and held there for a few minutes to ensure that any traces of previous crystal structure and residual stresses were removed. Subsequently, they were cooled rapidly to the crystallization temperature (varied between 140 - 145 °C) and quenched after 1 hour by placing them on a metal plate at room temperature. One of the samples crystallized at 140 °C for 1 hour was subsequently annealed at 150 °C for 1 hour. Prior to examination, the samples were etched for 1 hour in 1% solution of potassium permanganate in a mixture of sulfuric and orthophosphoric acid and immediately afterwards washed, according to the published procedures (43).

AFM images were taken in contact mode using a NanoScope® III instrument (Digital Instruments, Santa Barbara, California) equipped with J and D head, calibrated in x and y directions using a calibration grid and gold calibration grating. All scans were performed in air with Si_3N_4 Nanoprobe integrated microcantilevers with a nominal force constant of 0.38 N/m (NanoTips®, Digital Instruments). The scan rates selected were between 1.8 and 8 Hz, depending on the scan size. Imaging forces were minimized to 20 nN in order to obtain best

contrast. A minimal amount of 160 lamellar thickness were measured for each sample. The statistical analysis of the data (histograms of the thickness distribution, mean value of the lamellar thickness, and standard error (se)) was performed using Origin Microcal software.

Results and Discussion

At the investigated temperatures (140 - 145°C), ß-iPP crystallizes from the melt in the form of hedritic structures, which preserve a remarkably regular (flat-on) hexagonal shape during late stages of crystallization (36,42). In the different herdritic projections exposed to the sample surface, both flat-on and edge-on views of the lamellae can be observed (Figure 1 a, b).

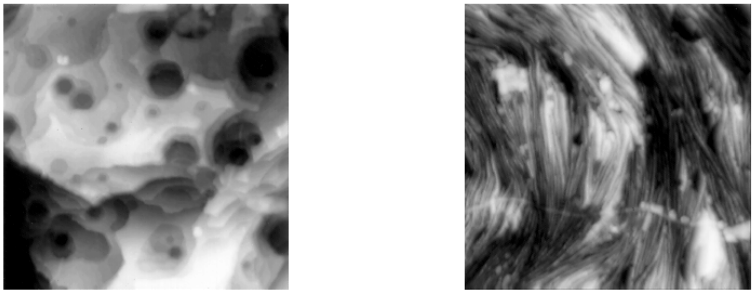

a) **b)**

Figure 1. AFM height images showing lamellae oriented a) flat-on, b) edge-on with respect to the examined surface. Image size 10μm x 10μm.

An abundance of hexagonally shaped spiral terraces can be seen in most of the flat-on views, associated with screw-dislocations etched down their axis. This allowed us to measure the step height between the successive layers of the screw-dislocations. Only layers parallel to the x-y scanning plane were chosen for measurements (Figure 2a). Otherwise, i.e. if the chosen layers were tilted, the value of the step height would have been overestimated. The value of the step height should correspond to the long period (thickness of the crystalline core 1_c + thickness of the amorphous layer 1_a). We assume that the permanganic etchant used removed the disordered layer covering the surface of the lamellae. It has been suggested that permanganic etchants can attack the fold surface, leaving only the crystalline core (43), consisting of an organized array of oxidized (mostly carboxyl) groups, which is very resistant to further oxidation. This accounts for the rate of erosion of the basal surface of the lamellae being much slower than that of the side faces. Sutton et al. (23) showed that etching times between 5 and 30 min. do not affect the measured value of the step height between the layers of spiral terraces in isotactic polystyrene crystals. In our experiments etching times of 20 min and 1 h 20 min showed a mean value of the lamellae thickness within the standard error of the lamellar thickness for the lamellae ecthed for 1h. It should be noted that in contrast to the sharp steps produced by etching, untreated crystal surfaces show round height profiles (44), which can lead to spurious values of lamellar thickness.

The lamellar thickness was also determined from the lamellae oriented edge-on with respect to the examined surface (Figure 2b). However in this case measured values correspond to the thickness of the crystalline core 1_c due to the surrounding amorphous

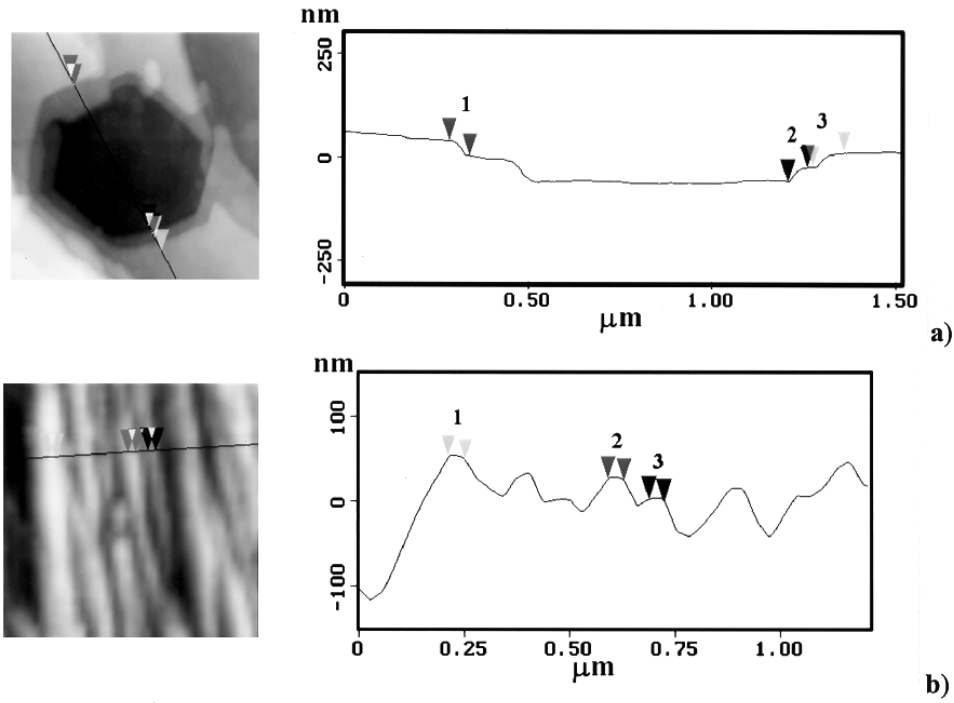

Figure 2. Section analysis of AFM images showing lamellar thickness for a sample of β-iPP crystallized at 140ºC for 1 h. a)flat-on lamellae. b)edge-on lamellae. Estimated lamellar thickness values for the pairs of markers shown: a) **1**- 36 nm, **2** - 33 nm, **3** - 34 nm; b) **1** - 40 nm, **2** - 37 nm, **3** - 35 nm.

layers being etched deeper, thus leaving the crystalline core to stand out prominently. One difficulty that might arise when measuring the thickness from the height profile of the edge-on oriented lamellae is due to AFM tip-sample interactions. The AFM tips used have a square-pyramidal shape which is rounded at the apex. The radius of this sphere seems to depend on the tips used, and is on the order of 20-50 nm (sometimes up to 100 nm). This makes it difficult to study steep features (such as edge-on lamellae, amorphous regions between which are deeper areas due to the etching) because they are generally imaged as rounded features due to tip-surface convolution during imaging. This effect can be reduced by deconvoluting the image obtained with the tip profile (45,46). Unfortunately, tip-sample interactions and tip-imaging artifacts can never be completely eliminated since during imaging of sharp, steep features there are always regions of the sample in the “shade” of the tip which cannot be probed. In our experiments the lamellar thickness was approximated by projecting the points at which the straight lines of the cross-section diverged from the curved “top” sections as shown in Figure 2b. Thus, those lamellae which gave a skewed profile in the height images were not included in our evaluation. These were assumed not to have grown perpendicular to the x-y scanning plane.

Histograms, showing the lamellar thickness distribution for the three investigated temperatures - 140, 143 and 145°C are shown in Figures 3a-c. Mean values obtained for the lamellar thickness and the standard error of the data are given in Table 1. The values follow the expected tendency of increase of the lamellar thickness with an increase in temperature.

However, the difference between the detected lamellar thickness at different temperatures is relatively small. This result can be explained by the isothermal lamellar thickening that takes place during isothermal crystallization and by the fact that nucleation density can have an effect on the determined lamellar thickness (17). For a range of materials with different nucleation densities crystallized at the same temperature and time, the average age of the lamellae can vary significantly. Therefore, the degree of thickening is expected to be different and it is anticipated that older lamellae will thicken more. It has been observed that samples with higher nucleation density consistently produce thicker lamellae for the same crystallization conditions (17). In our case the nucleation density dramatically decreases with an increase of temperature between 140 to 145 °C, which can be detected from optical microscopy observations. At the relatively short crystallization time of 1 hour applied here the majority of the lamellae formed at 140 °C will be older in comparison to those formed at higher temperature and therefore have more time to thicken.

It should be noted that in the situation where samples are partially crystallized and then quenched, a bimodal lamellar thickness distribution is observed; one population of lamellae being formed during the isothermal crystallization, and the other developing during quenching (18). In our case, quenching caused a so-called growth halo to be

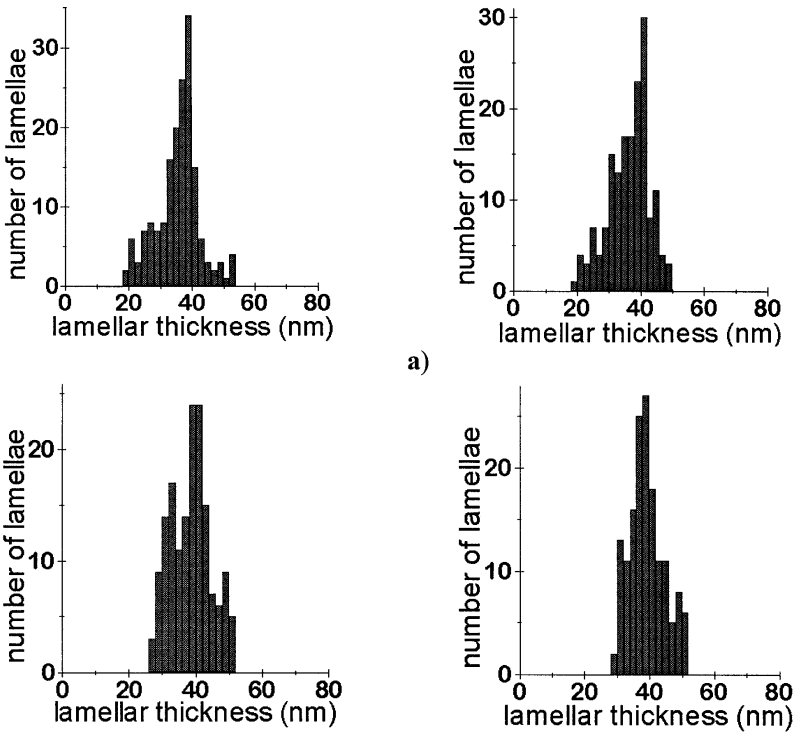

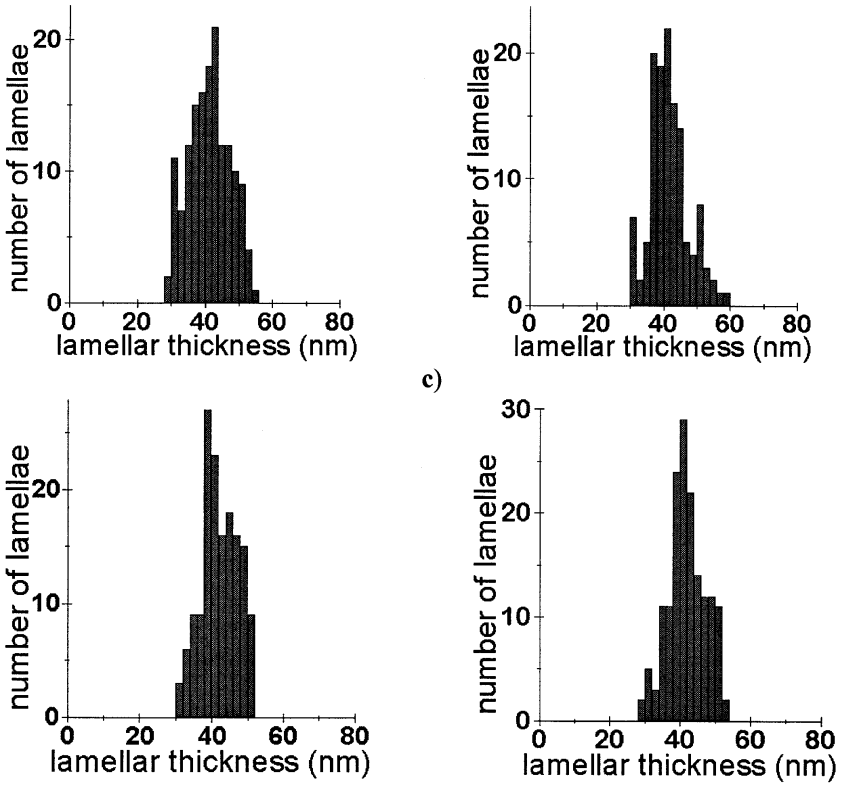

Figure 3. Histograms showing lamellar thickness distributions for β-iPP crystallized for 1 hour at: a) 140°C, b) 143°C, c) 145°C, d) 140°C, and annealed for 1 hour at 150°C. Left-hand histograms are based on lamellar thickness values obtained from flat-on views, right hand histograms - on lamellar thickness values obtained from edge-on views.

Table 1

Crystallization temperature	Lamellar thickness - mean value (nm)	se
140°C		
flat-on views	35.1	0.5
edge-on views	35.8	0.5
143 °C		
flat-on views	38.1	0.5
edge-on views	38.6	0.5
145 °C		
flat-on views	40.8	0.5
edge-on views	41.2	0.5
140/150 °C		
flat-on views	41.7	0.4
edge-on views	41.9	0.4

formed around the hedrite. The lamellae in the halo were generally thinner and were not included in the present results, because the average measured thickness did not change significantly with the crystallization temperature. We did not observe any population of thinner lamellae inside the hedritic structures.

Annealing for 1 hour at 150°C of the sample crystallized at 140°C causes the lamellar thickness distribution to be shifted towards larger values (Figure 3d). The distribution also becomes narrower. Presumably at 150 °C the temperature is too high and nucleation of new ß lamellae does not occur. Therefore, the lamellae that were formed at 140 °C are responsible for the observed thickening caused by

chain refolding. To explain the narrowing of the thickness distribution, we assume that after a certain size the increase of the lamellar thickness becomes slower. Thus, the thinner portion of the lamellae formed at 140 °C contributes to the increase of the lamellar thickness more than the old lamellae already thickened at 140 °C.

Comparison between the lamellar thickness measured from the flat-on and edge-on views shows that the latter always appear slightly higher. However, the thickness determined from the edge-on views corresponds to the crystalline core 1_c and therefore should be lower than the value determined from the flat-on view consistent with the long period 1_a. Therefore, the thickness measured from the edge-on views is slightly overestimated, most probably due to the convolution of the tip shape with the surface features, as discussed previously.

It was already pointed out that for an AFM measurement the lamellae have to be in a favourable orientation relative to one of the scan directions (i.e. not distorted or tilted with respect to the sample surface). This is also a problem for measurements of the lamellar thickness by electron microscopy, and can lead to erroneous results if not taken into account. Our experiments have demonstrated that AFM has the advantage of revealing the lamellar orientation with respect to the surface, so measurements can be restricted to lamellae with favourable orientations.

Conclusions

Measurements of lamellar thickness and distribution in ß-PP crystallized from the melt at high temperatures has been performed. Average lamellar thickness was found to be dependent not only on the crystallization temperature, but also on factors such as nucleation density and lamellar thickening taking place during the isothermal crystallization. Obtained lamellar thickness distributions were broad. Annealing at temperatures higher than the upper limit of nucleation of ß-form resulted in an increase of the average lamellar thickness and narrowing of the distribution.

The use of AFM for quantitative evaluation of polymer morphology has been demonstrated as well. It proved to be of value for structural observations in real space and for identifying lamellar profile and orientation with respect to the examined surface.

Acknowledgment: Financial support given by “Deutsche Forschungsgemeinschaft” and University of Twente is greatly appreciated. The authors thank Mr. L. O’Connor for his help with the editing of the manuscript.

References:

1. Mandelkern L (1979) Faraday Soc Discuss 68: 310
2. Bassett DC, Hodge AM, Olley RH (1979) Faraday Soc Discuss 68: 218
3. Brown RG, Eby R K (1964) J Appl Phys 35: 1156
4. Strobl GR (1972) Kolloid Z Z Polym 250: 1039
5. Crist B, Morosoff N (1973) J Polym Sci Polym Phys Ed 11: 1023
6. Ruland W (1977) Colloid Polym Sci 255: 417
7. Strobl GR, Schneider MJ, Voigt-Martin IG (1980) J Polym Sci Polym Phys Ed 18: 1361
8. Voigt-Martin IG, Alamo R, Mandelkern L (1986) J Polym Sci Polym Phys Ed 24: 1283
9. Schaufele RF, Shimanouchi T (1967) J Chem Phys 47: 3605
10. Olf HG, Peterlin A, Peticolas WL (1974) J Polym Sci Polym Phys Ed 12: 359
11. Koenig JL, Tabb DL (1974) J Macromol Sci B9: 141

12. Folkes MJ, Keller A, Stejny J, Fraser GV, Hendra PJ, Goggin PL (1975) Colloid Polym Sci 13: 341
13. Voigt-Martin IG (1980) J Polym Sci Polym Phys Ed 18:1513
14. Bassett DC (1981) Principles of polymer morphology. Cambridge University Press, Cambridge
15. Martines-Salazar J, Keller A, Cagiao ME, Rueda DR, Balta, Calleja FJ (1983) Colloid Polym Sci 261: 412
16. Voigt-Martin IG (1985) Adv Polym Sci 67:194.
17. Dlugosz J, Frazer GV, Grubb D, Keller A, Odell JA (1976) Polymer 17: 471
18. Voigt-Martin IG, Mandelkern L (1989) J Polym Sci Polym Phys Ed 27: 967
19. Voigt-Martin IG, Stack GM, Peacock AJ, Mandelkern L, (1989) J Polym Sci Polym Phys Ed 27: 957
20. For a recent review see: Magonov SN, Wangbo MH (1996) Surface analysis with STM and AFM. VHC, Weinheim
21. Patil R, Kim S-J, Smith E, Reneker DH, Weisenhorn AL (1990) Polym Commun 31: 455
22. Snetivy D, Vancso GJ (1992) Polymer 33: 432
23. Sutton SJ, Izumi K, Miyaji H, Fukao K, Miyamoto Y (1996) Polymer 24: 5529
24. Schönherr H, Snetivy D, Vancso GJ (1993) Polym Bull 30: 567
25. Vancso GJ, Nisman R, Snetivy D, Schönherr H, Smith P, Ng C, Yang H (1994) Coll Surf A87: 263
26. Zhou H, Wilkes GL (1997) Polymer 38: 5735
27. Varga J (1992) J Mater Sci 27: 2557
28. Fujiwara Y, Goto T, Yamashita Y (1987) Polymer 28: 1253
29. Binsbergen FL, de Lange BGM (1968) Polymer 9: 23
30. Norton DR, Keller A (1985) Polymer 26: 704
31. Lotz B, Wittmann JC (1986) J Polym Sci Polym Phys Ed 24: 1541
32. Wittmann JC, Lotz B (1990) Progr Polym Sci 15: 909
33. Bassett DC, Olley RH (1984) Polymer 25: 935
34. Olley RH, Bassett DC (1989) Polymer 30: 399
35. Aboulfaraj M, Ulrich B, Dahoun A, G'Sell C (1993) Polymer 34: 4817
36. Varga J, Ehrenstein GW (1997) Colloid Polym Sci 275: 511
37. Varga J (1995) Crystallization, melting and supermolecular structure of isotactic polypropylene. In: Karger-Kocsis J (ed) Polypropylene: structure, blends and composites. Chapman&Hall, London,vol 1, pp 57-115.
38. Turner-Jones A, Cobbold AJ (1968) J Polym. Sci B6: 539
39. Meille SV, Fero DR, Brückner S, Lovinger AJ, Padden FJ (1994) Macromolecules 27: 2615.
40. Lotz B, Kopp S, Dorset D (1994) C R Acad Sci Paris 319IIb: 187
41. Varga J, Schulek-Toth F, Pati Nagy M (29/4/1992) Hungarian Patent 209132
42. Trifonova D, Varga J, Ehrenstein GW, Vancso GJ (1996) ACS Polymer Preprints 37: 563
43. Olley R (1986) Sci Progr Oxf 70: 17
44. Motomatsu M, Nie H-Y, Mizutani W, Tokumoto H (1996) Polymer 37: 183
45. Grütter P, Zimmermann-Edling W, Brodbeck D (1992) Appl Phys Lett 60: 2741
46. Markiewicz P, Goh MC (1994) Langmuir 10: 5